ACS SyntheticBiology

Research Article

pubs.acs.org/synthbio

Engineering Hybrid Chemotaxis Receptors in Bacteria

Shuangyu Bi, Abiola M. Pollard, Yiling Yang, Fan Jin, and Victor Sourjik*

Max Planck Institute for Terrestrial Microbiology & LOEWE Center for Synthetic Microbiology (SYNMIKRO), Marburg, Germany

Supporting Information

ABSTRACT: Most bacteria use transmembrane sensors to detect a wide range of environmental stimuli. A large class of such sensors are the chemotaxis receptors used by motile bacteria to follow environmental chemical gradients. In *Escherichia coli*, chemotaxis receptors are known to mediate highly sensitive responses to ligands, making them potentially useful for biosensory applications. However, with only four ligand-binding chemotaxis receptors, the natural ligand spectrum of *E. coli* is limited. The design of novel chemoreceptors to extend the sensing capabilities of *E. coli* is therefore a critical aspect of chemotaxis-based biosensor development. One path for novel sensor design is to harvest the large natural diversity of chemosensory functions found in bacteria by creating hybrids that have the signaling domain from *E. coli* chemotaxis receptors and sensory domains from other species. In this work, we demonstrate that the *E. coli* receptor Tar can be successfully combined with most typical sensory domains found in chemotaxis receptors and in evolutionary-related two-component histidine kinases. We show that such functional hybrids can be generated using several different fusion points. Our work further illustrates how hybrid receptors could be used to quantitatively characterize ligand specificity of chemotaxis receptors and histidine kinases using standardized assays in *E. coli*.

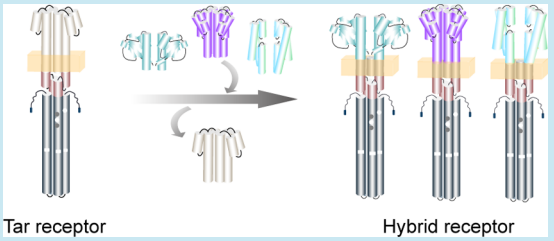

KEYWORDS: *hybrid chemoreceptors, extracellular sensory domain, chemotaxis, methyl-accepting chemotaxis protein, histidine kinase, ligand*

Bacteria have evolved the ability to detect a wide range of environmental signals by using diverse sensory systems, allowing them to survive and grow under rapidly changing conditions.[1,2] Utilizing this diversity for engineering bacterial sensory systems to recognize specific molecules of interest would be a key step in biosensory applications.[2] One of the most prominent prokaryotic sensory systems is the chemotaxis network, which is present in most motile bacteria and archaea, enabling navigation in environmental gradients of various chemicals.[1,3−5] Although chemoeffector spectra of only a few bacteria have been characterized, chemotaxis is known to play an important role not only in locating nutrients and avoiding harmful chemicals[6] but also in bacterial communication,[7] degradation of xenobiotic compounds,[8] and in host infection.[9]

The most studied model of bacterial chemotaxis is *E. coli*, whose chemotaxis network consists of five chemotaxis receptors (also called methyl-accepting chemotaxis proteins) and six cytoplasmic signaling proteins: a histidine autokinase CheA, an adaptor CheW, a response regulator CheY, a methyltransferase CheR, a methylesterase CheB, and a phosphatase CheZ.[10−12] These signaling components work in coordination to process chemotactic stimuli and to control the rotation of the flagellar motors. The activity of receptor-associated CheA is inhibited when attractant binds to the receptor, whereas repellent binding enhances the activity. CheA subsequently passes the phosphoryl group to CheY, which controls cell swimming; dephosphorylation of CheY is performed by CheZ. After the initial response, cells can gradually adapt to background stimulation by adjusting the levels of receptor methylation *via* CheR and CheB. Thereby, CheR preferentially methylates receptors that have inactive (kinase-inhibitory) conformations, whereas CheB demethylates active receptors, respectively increasing or decreasing their activity.

Four ligand-binding chemotaxis receptors in *E. coli*, Tsr, Tar, Trg, and Tap, all have the same topology[13] and can be divided into a transmembrane sensing module, a signal conversion module, and a kinase control module.[12] The transmembrane sensing module is composed of an extracellular sensory domain and two transmembrane helices (TM1 and TM2). When ligand binds to the pocket inside the sensory domain, it triggers conformational changes in the TM region. This conformational signal is further transduced to the cytoplasmic part of the receptor by the signal conversion module, consisting of a HAMP domain. The kinase control module contains a methylation helix (MH) bundle, a flexible bundle, and a protein contact region that interacts with the kinase and regulates its activity. Chemotaxis receptors can differ in their domain organization,[13] but the topology characteristic to *E. coli* ligand-binding receptors with a clearly identifiable extracellular sensory domain is found in the majority of bacteria. Except for a few examples, the ligand specificity of different sensory domains remains unknown. Most of these sensory domains, however, can be fit into a relatively small number of common structural classes. According to the most common classification, these include four-helix bundle,[14] single PhoQ-DcuS-CitA (PDC),[15] double PDC,[15] helical

Received: February 7, 2016

DOI: 10.1021/acssynbio.6b00053
ACS Synth. Biol. XXXX, XXX, XXX−XXX

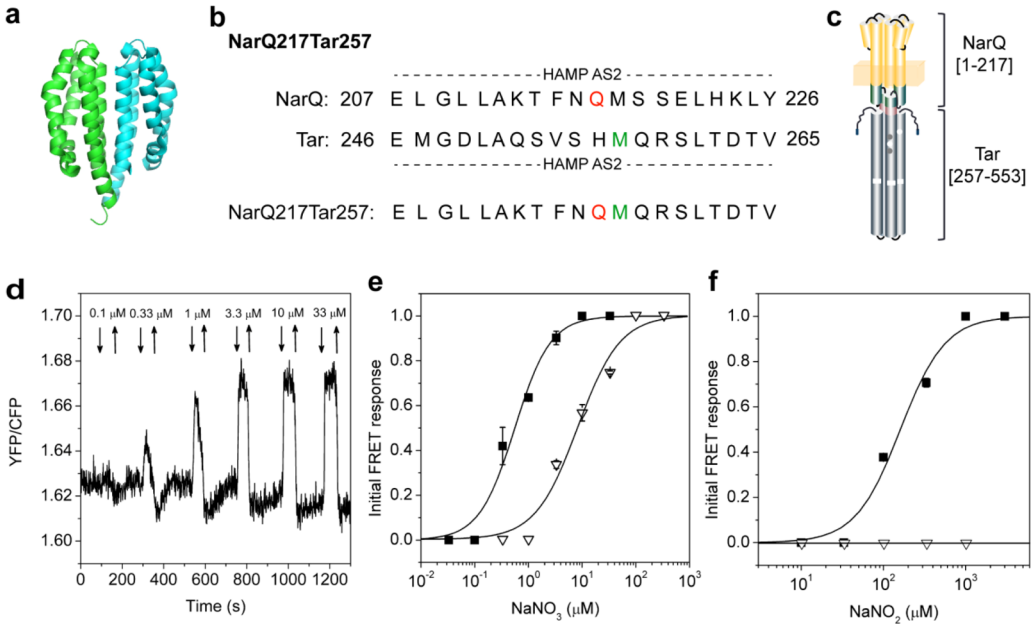

Figure 1. Construction and characterization of the NarQ-Tar hybrid. (a) Structure of a four-helix bundle domain (the sensory domain of NarX from *E. coli*, PDB ID: 3EZH). Here and in subsequent figures, the two monomers that form the sensory domain are shown in different colors. (b) Sequence alignment for NarQ and Tar with the fusion sites between NarQ and Tar shown in red and green, respectively, and the sequence of the hybrid receptor shown below. (c) Cartoon representation of the hybrid NarQ217Tar257. (d) FRET responses of buffer-adapted *E. coli* cells expressing NarQ-Tar as the sole receptor upon stepwise addition (down arrow) and subsequent removal (up arrow) of the indicated concentrations of $NaNO_3$. (e) The corresponding amplitudes of the initial FRET response (change in the YFP/CFP ratio after stimulation and before adaptation) for NarQ-Tar were plotted as a function of stepwise changes in concentration of $NaNO_3$ in buffer (closed squares) or in the presence of 10 mM $NaNO_2$ (open triangles). (f) The dose response of NarQ-Tar to $NaNO_2$ in buffer (closed squares) or in the presence of 100 μM $NaNO_3$ (open triangles). In e and f, the data were normalized to the saturated response. Error bars indicate the standard errors of two independent experiments; wherever invisible, error bars are smaller than the symbol size.

biomodular (HBM),[16] and nitrate and nitrite sensing (NIT).[17] The same domains are also found in bacterial two-component histidine kinases (HKs), which are evolutionarily related to the chemotaxis receptors but regulate gene expression instead of motility.

The variety of sensory domains that can accommodate different types of ligands, as well their modularity, make chemoreceptors highly attractive for biosensor engineering.[2,18−20] For a given bacterium, the ligand range of the chemotaxis system can be greatly expanded through the construction of hybrid receptors that utilize extracellular sensory domains from "donor" chemotaxis receptors or HKs found in other species. A prerequisite for employing this strategy is that the sensory domains with different structures—potentially sensing different types of ligands—can be reliably coupled to the cytoplasmic part of another ("recipient") receptor. Previous studies have reported several examples of such functional hybrids between different chemotaxis receptors from the same species, such as Tsr-Tar,[21] Trg-Tsr,[22] and Tap-Tar[23] in *E. coli* and McpB-McpC in *Bacillus subtilis*,[24] as well as hybrids between PctA, PctB, and PctC from *Pseudomonas aeruginosa*[25,26] or McpG from *Pseudomonas putida* and *E. coli* Tar.[26] Furthermore, hybrids of *E. coli* HK NarX with Tar[27] or receptor FrzCD from *Myxococcus xanthus*[28] were also constructed. However, the rational design of functional receptor hybrids remains a challenging task.[2] One problem is the intrinsically high sensitivity of chemotaxis receptors to small conformational perturbations, which is important for signal transduction. This means that even modest perturbations due to an incorrect fusion of a new sensory domain might bias a hybrid receptor into a locked-on or -off conformation/activity, although these changes might in part be compensated by the receptor methylation system. Besides such extreme activity bias, nonfunctional hybrids between different receptors can also result from the failure of signal transmission from the sensory to the signaling domain.

In this work, we demonstrate the successful construction of hybrid receptors, fusing the most common extracellular sensory domains (four-helix bundle, HBM, NIT, single PDC, and double PDC) with the cytoplasmic signaling domain of *E. coli* Tar. By systematically testing different fusion sites, we explored how to choose the optimal fusion point(s) for hybrid receptors. We further show that hybrid receptors can be used to identify novel ligands of receptors from organisms other than *E. coli*. Our study provides important insights for engineering of chemoreceptors with a wide range of specificities that could have many applications in biosensing.

RESULTS

Four-Helix Bundle Domain Hybrid Receptor. To systematically explore the construction of chemoreceptors with different sensory domains, we started with a four-helix bundle domain that is ubiquitous in prokaryotic signaling proteins.[14] The sensory domains of *E. coli* chemotaxis receptors belong to TarH, a pseudo four-helix bundle domain,[29,30] and a number of hybrids between *E. coli* receptors have been reported previously with fusions at different sites: above TM2,[6] in TM2,[21,31] in the HAMP domain,[22,23,32,33] after the HAMP domain,[33] and in the kinase control module.[32,33] To verify our capability to construct other hybrids with a four-helix bundle domain, we used the sensory domain of histidine kinase NarQ (Figure 1a), which senses nitrate and nitrite[34] and regulates expression of anaerobic respiratory genes.[35] We chose the fusion point within the second

DOI: 10.1021/acssynbio.6b00053
ACS Synth. Biol. XXXX, XXX, XXX−XXX

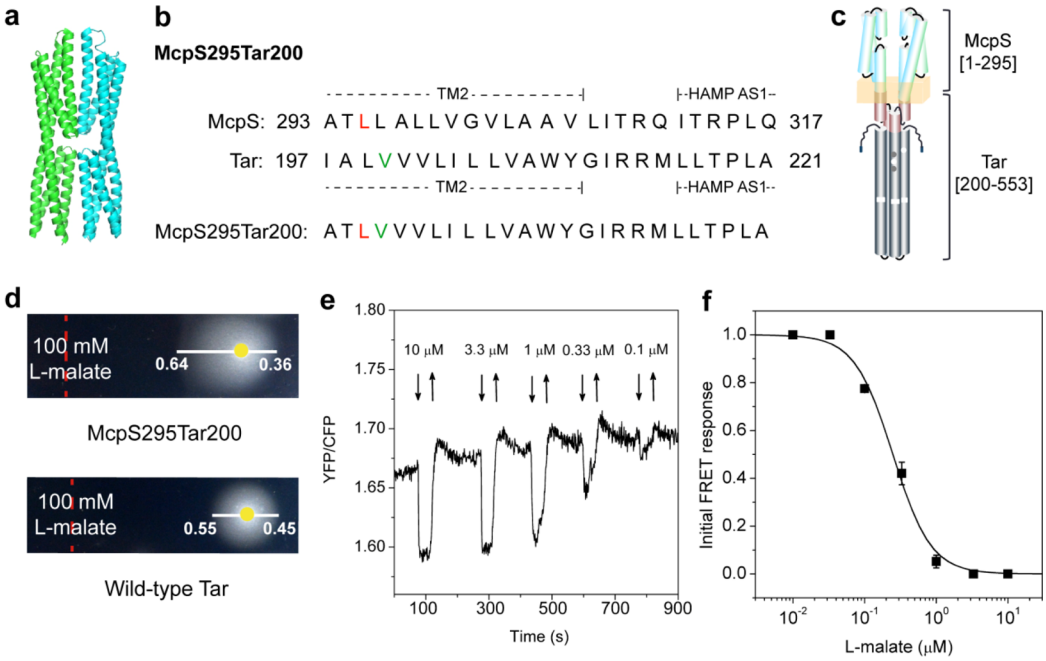

Figure 2. Construction and characterization of the McpS-Tar hybrid. (a) Structure of an HBM domain (the sensory domain of McpS from *P. putida*, PDB ID: 2YFA). (b) Sequence alignment for McpS, Tar, and the hybrid receptor of the two; fusion sites between McpS and Tar are shown in red and green, respectively. (c) Cartoon representation of the hybrid McpS295Tar200. (d) The response of the McpS-Tar hybrid and wild-type Tar to L-malate measured by an agar plate assay. Sites of the ligand source and inoculated cells are shown by a red dotted line and by a yellow dot, respectively. Spreading of cells toward or away from the ligand source is indicated by the white line. (e, f) Example of a FRET measurement of buffer-adapted *E. coli* cells expressing McpS-Tar as the sole receptor responding to stepwise addition (down arrow) and subsequent removal (up arrow) of the indicated concentrations of L-malate (e) and the corresponding dose−response curve (f) analyzed and plotted as in Figure 1.

helix (AS2) of the HAMP domain, guided by the previously reported functional hybrid between the closely related HK NarX and Tar,[27] and using ClustalW[36] for sequence alignment (Figure 1b). The resulting hybrid NarQ[1−217]-Tar[257−553] (NarQ217Tar257) connects the extracellular sensory domain, the two TM helices, and part of the HAMP domain from NarQ to the rest of the HAMP domain and the kinase control module of Tar (Figure 1c). The coding sequence of this hybrid was cloned into an expression vector inducible by sodium salicylate[37] (see Methods and Table S1), and the expression of the construct was verified using immunoblotting (Figure S1). The regulation of the chemotaxis pathway activity by the hybrid receptor was characterized using a previously described pathway activity reporter based on fluorescence (Förster) resonance energy transfer (FRET).[38,39] This assay allows monitoring of the phosphorylation-dependent interaction between CheY fused to yellow fluorescent protein (CheY-YFP) and its phosphatase CheZ fused to cyan fluorescent protein (CheZ-CFP) and thus measurements of the intracellular changes in the pathway activity due to chemotactic stimulation with increased CheA activity resulting in a higher ratio of YFP/CFP fluorescence. The response of NarQ217Tar257 to the NarQ ligands nitrate and nitrite was studied in strain VS181[39] that lacks all native receptors but possesses the intact receptor methylation system (Table S1). The same approach was also used for the characterization of all other hybrids (see below). FRET measurements demonstrated that the NarQ-Tar hybrid receptor mediates repellent responses to $NaNO_3$ (nitrate) and $NaNO_2$ (nitrite) (Figure 1d−f and Figure S2a) with the initial rapid increase in the kinase activity (corresponding to the increase in YFP/CFP ratio) upon stimulation, which is followed by slow methylation-dependent adaptation. These responses were similar to those observed for the Tar-mediated response to repellents (e.g., $NiCl_2$) using FRET.[38] The responses of NarQ-Tar showed different dose dependences for nitrate and nitrite with EC_{50} values of 0.56 ± 0.08 and 161 ± 21 μM, respectively (Figure 1e and f). These responses were specific because the wild-type Tar did not respond to $NaNO_3$ at any of the given concentrations, and a response to $NaNO_2$ was observed only at the highest concentration tested (Figure S2b). To test if nitrate and nitrite competitively bind to the same binding pocket of NarQ, we adapted the hybrid to a saturating level of one ambient ligand and measured the response to the other. The binding of nitrate and nitrite to NarQ-Tar was apparently competitive because adaptation to 100 μM $NaNO_3$ completely inhibited the response to $NaNO_2$, whereas adaptation to 10 mM $NaNO_2$ raised the EC_{50} of the response to $NaNO_3$ to 8.2 ± 1.4 μM (Figure 1e and f). Notably, it was previously shown that such mutual inhibition is only observed for the competitive binding of the two ligands, whereas adaptation to a ligand that signals through the same receptor *via* a different mechanism has no effect on the response.[40]

HBM Domain Hybrid Receptor. The HBM domains are found in chemotaxis receptors and HKs from bacteria and archaea.[16] Its structure, exemplified by McpS from *P. putida* KT2440,[41] contains six helices arranged into two modules (Figure 2a). The membrane-proximal module was shown to bind several TCA cycle intermediates, such as malate, succinate, and citrate,[41,42] whereas the membrane-distal module of McpS was proposed to sense acetate as a ligand.[41] For the constructuction of an McpS-Tar hybrid, the extracellular sensory domain of McpS was combined with Tar within the TM2 region to yield McpS[1−295]-Tar[200−553] (McpS295Tar200) (Figure 2b and c). *E. coli* UU1250[43] (Table S1) expressing this hybrid as the

DOI: 10.1021/acssynbio.6b00053
ACS Synth. Biol. XXXX, XXX, XXX−XXX

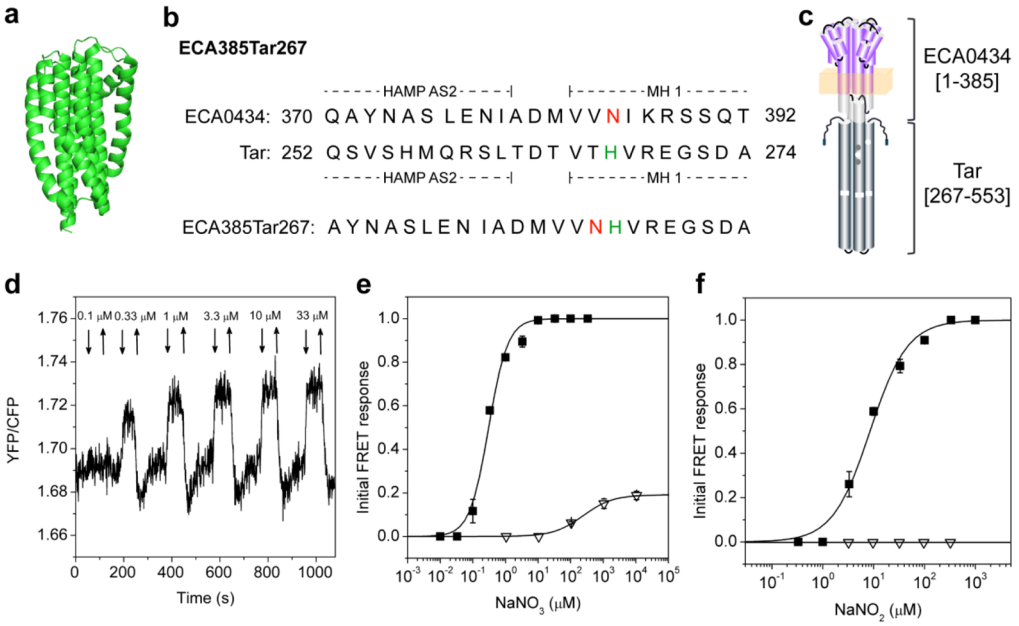

Figure 3. Construction and characterization of the ECA0434-Tar hybrid. (a) Structure of a monomer of the NIT domain of NasR from *K. oxytoca* (PDB ID: 4AKK). (b) Sequence alignment for ECA0434 and Tar; fusion sites between ECA0434 and Tar are shown in red and green, respectively. (c) Cartoon representation of the hybrid ECA385Tar267. (d) FRET responses of buffer-adapted *E. coli* cells expressing ECA0434-Tar as the sole receptor upon stepwise addition (down arrow) and subsequent removal (up arrow) of the indicated concentrations of $NaNO_3$. (e) Corresponding dose response of ECA0434-Tar to $NaNO_3$ in buffer (closed squares) or in the presence of 1 mM $NaNO_2$ (open triangles). (f) The dose response of ECA0434-Tar to $NaNO_2$ in buffer (closed squares) or in the presence of 100 μM $NaNO_3$ (open triangles). Dose−response curves were analyzed and plotted as in Figure 1.

sole receptor showed a good attractant response to L-malate in the agar plate assay, in which directional spreading of swimming cells occurs along a pre-established gradient of chemoeffector within the agar (Figure 2d). This was confirmed by the FRET measurement, which showed the EC_{50} of response to L-malate to be 0.25 ± 0.02 μM (Figure 2e and f). Besides L-malate, the hybrid also mediated less sensitive attractant responses to succinate (EC_{50} = 2.7 ± 0.2 μM) and citrate (EC_{50} = 35.7 ± 2.0 μM) (Figure S3a and b). This order of sensitivity was consistent with the previously measured binding affinities of McpS for L-malate (8.5 μM), succinate (82 μM), and citrate (109 μM),[42] although the EC_{50} obtained from the *in vivo* FRET measurements are lower by more than an order of magnitude. This difference could be explained by the signal amplification within the receptor clusters *in vivo*. Notably, L-malate and succinate also elicited FRET response in cells expressing the wild-type Tar but only at significantly higher doses (Figure S3c); no response to citrate was observed (Figure S3c). However, our hybrid showed no response to acetate below 300 μM, whereas at higher concentrations McpS-Tar and Tar both showed similar repellent responses (Figure S3d), making it impossible to confirm acetate sensing by McpS.

NIT Domain Hybrid Receptor. The NIT domain is prevalent in prokaryotic intracellular transcription antitermination regulators, HKs, chemotaxis receptors, and diguanylatecyclases and diesterases.[17] The structure of the NIT domain, determined for the NasR protein from *Klebsiella oxytoca*,[44] contains nine α-helices, eight of which form a pair of four-helix bundles[34,44] (Figure 3a). We made a hybrid using the extracellular NIT sensory domain of the putative chemotaxis receptor ECA0434 from *Pectobacterium atrosepticum* strain SCRI 1043. This receptor contains two transmembrane helices and a HAMP domain, as predicted by the SMART online server (http://smart.embl.de).[45] The hybrid ECA0434[1−385]-Tar[267−553] (ECA385Tar267) was constructed using fusion at the position after the HAMP domain of ECA0434/at the beginning of MH1 of Tar (Figure 3b and c). Cells expressing this hybrid receptor had a highly sensitive repellent response to $NaNO_3$ in FRET measurements with an EC_{50} of 0.31 ± 0.03 μM (Figure 3d and e). It also mediated a less sensitive repellent response to $NaNO_2$ with an EC_{50} of 8.5 ± 0.9 μM (Figure 3f and Figure S4), confirming that the NIT domain confers nitrate and nitrite sensitivity. When adapted with 1 mM $NaNO_2$ or 100 μM $NaNO_3$, the cells were dramatically inhibited in responding to $NaNO_3$ or $NaNO_2$, respectively, indicating that nitrate and nitrite compete for the same binding site of ECA0434 (Figure 3e and f).

Single PDC Domain Hybrid Receptor. The single PDC domain widely exists in chemotaxis receptors and HKs.[15] In the Pfam library, it is also grouped into the Cache_3 domain. The single PDC domain has one Per/ARNT/Sim (PAS)-like $\alpha+\beta$ module that was structurally characterized for HKs PhoQ, DcuS, and CitA[15,46−48] (Figure 4a). Here, we focused on *E. coli* CitA, where this domain is used to sense citrate and to mediate signals to a C-terminal HK part composed of a catalytic domain and a dimerization domain.[48,49] CitA does not use a HAMP domain to mediate signal transduction and shows no evolutionary conservation with Tar. We thus decided to combine CitA and Tar at the positions above the HAMP domain: either above the two TM helices or in TM2. For the CitA-Tar hybrid with the fusion site above the two TM helices, we conducted the sequence alignment and secondary structure prediction using PSIPRED V3.3 (http://bioinf.cs.ucl.ac.uk/psipred/)[50] to select the fusion residues in the N- and C- terminals of the CitA sensory domain (Figure 4b). Cells expressing the hybrid Tar[1−43]-CitA[55−173]-Tar[184−553] (Tar43CitA55Tar184) had an attractant response to citrate (Figure 4c and Figure S5a) with an EC_{50} of 1.1 ± 0.1 μM. It also showed a weaker attractant response to

DOI: 10.1021/acssynbio.6b00053
ACS Synth. Biol. XXXX, XXX, XXX−XXX

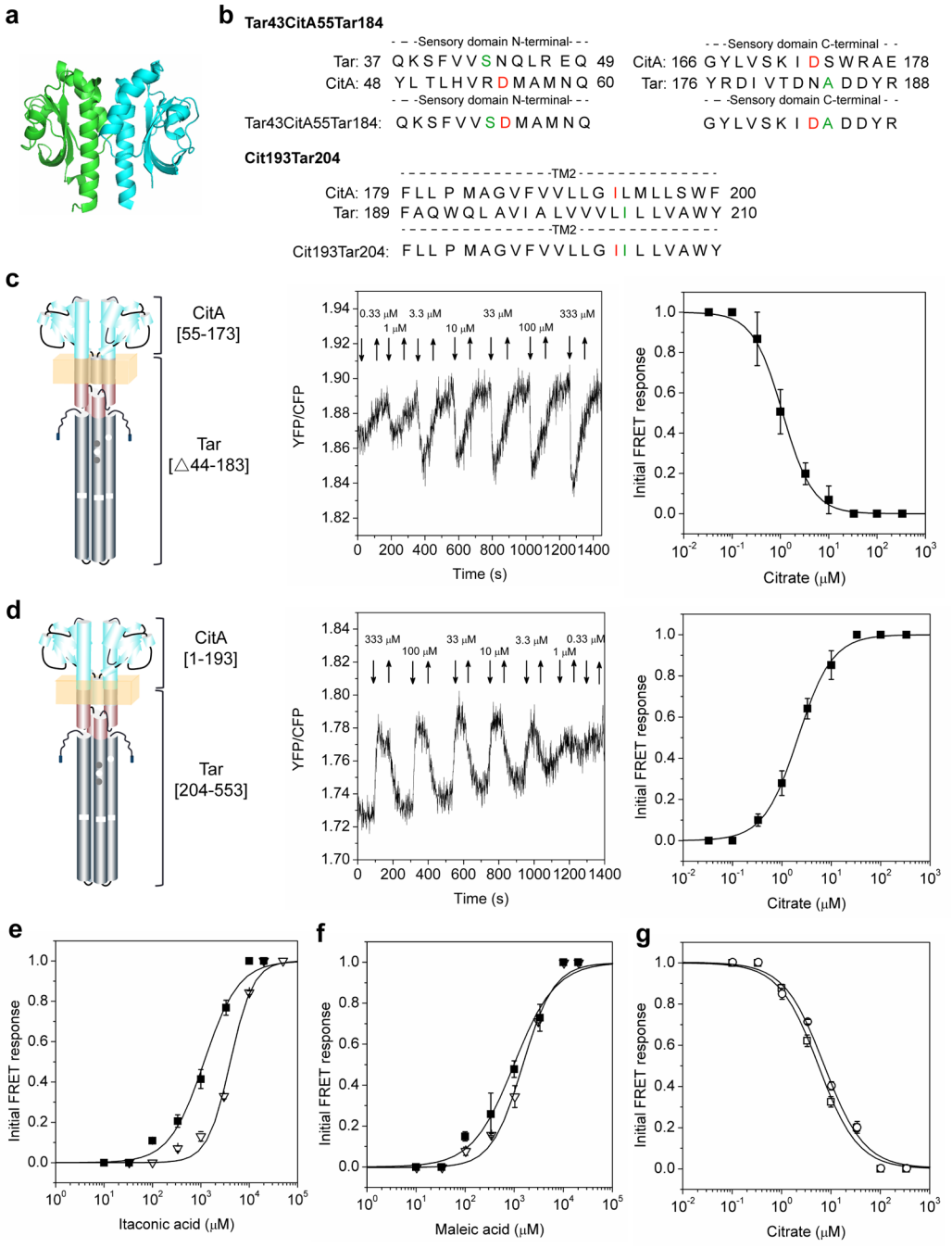

Figure 4. Construction and characterization of the CitA-Tar hybrids. (a) Structure of a single PDC domain (the sensory domain of histidine kinase CitA from *Klebsiella pneumoniae*, PDB ID: 2J80). (b) Sequence alignment for CitA and Tar in hybrids Tar43CitA55Tar184 and CitA193Tar200; fusion sites between CitA and Tar are shown in red and green, respectively. (c, d) FRET measurements and response curves of buffer-adapted *E. coli* cells expressing Tar43CitA55Tar184 (c) or CitA193Tar200 (d) as the sole receptor at the indicated concentrations of citrate. (e, f) The dose response of Tar43CitA55Tar184 to itaconic acid (e) or maleic acid (f) in buffer (closed squares) or in the presence of 2 mM citrate (open triangles). (g) Dose–response curve of Tar43CitA55Tar184 to citrate in the presence of 10 mM itaconic acid (open squares) or maleic acid (open circles). Dose–response curves were analyzed and plotted as in Figure 1.

isocitrate with an EC_{50} of 43.5 ± 4.4 μM (Figure S5b). This is comparable to the *in vitro* measured binding affinities of citrate and isocitrate to CitA (0.15–1.0 μM for citrate and ~15 μM for isocitrate).[49] The fusion within TM2 was constructed based on the alignment of the aromatic anchors (Figure 4b). This fusion was also functional, and the FRET measurements showed that the hybrid CitA[1–193]-Tar[204–553] (Cit193Tar204) sensed citrate as a repellent (Figure 4d) with an EC_{50} of 2.1 ± 0.1 μM. The responses of these two hybrids are specifically mediated by the ligand-binding pocket of CitA because Tar did not respond to citrate or isocitrate (Figure S3c and Figure S5c). Interestingly, Cit193Tar204 and Tar43CitA55Tar184 have opposite responses to citrate. This may result from the two hybrids adopting different conformations, such that the same signal input from the sensory domain induces an opposing conformational change in the HAMP domain of the receptor.

We have further tested several additional compounds and discovered that, besides reported C6 acids (citrate, isocitrate, and

DOI: 10.1021/acssynbio.6b00053
ACS Synth. Biol. XXXX, XXX, XXX–XXX

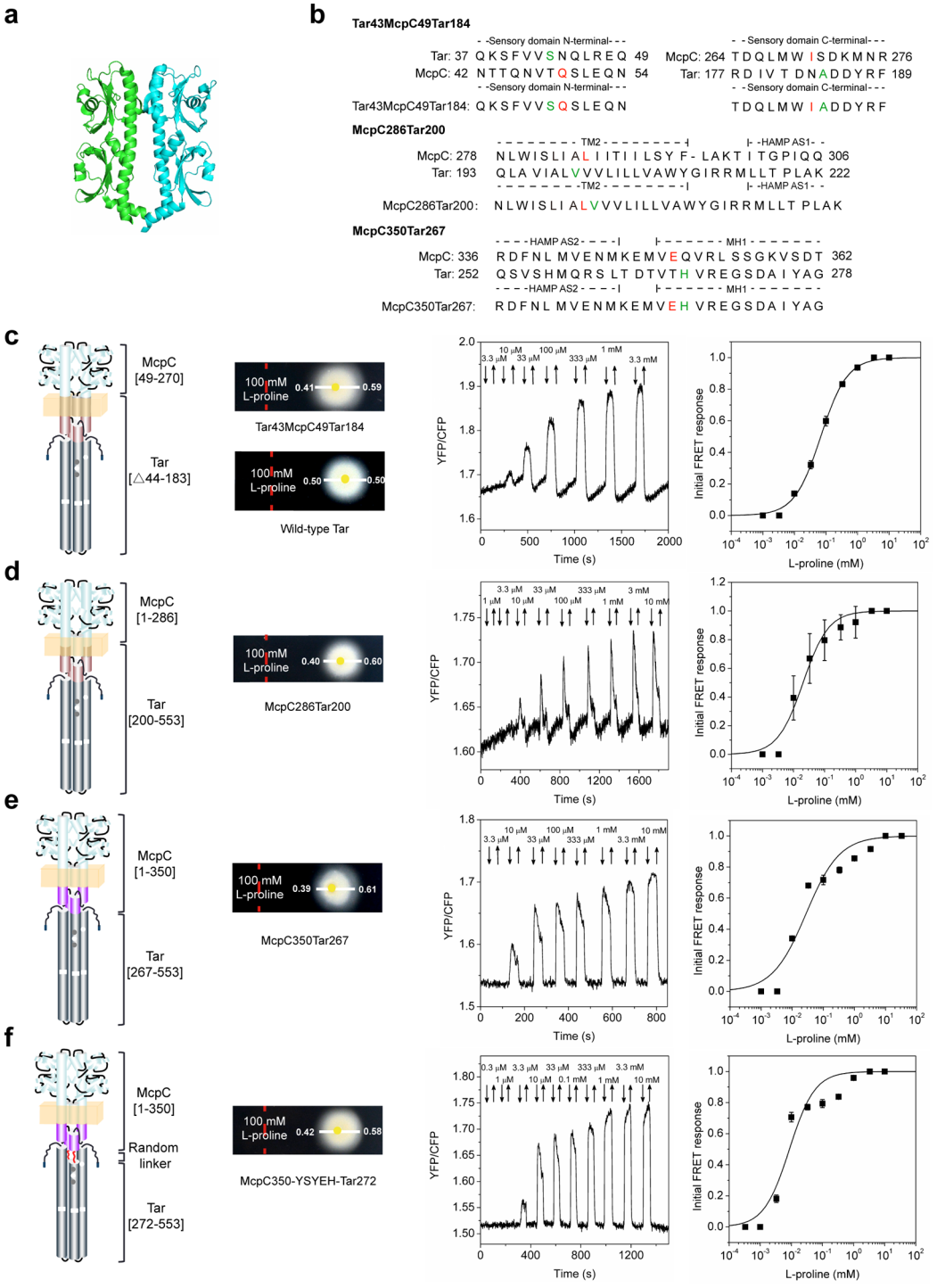

Figure 5. Construction and characterization of the McpC-Tar hybrids. (a) Structure of a double PDC domain (the sensory domain of a chemotaxis receptor from *Vibrio cholerae*, PDB ID: 3C8C). (b) Sequence alignment for the McpC and Tar components in hybrids Tar43McpC49Tar184, McpC286Tar200, and McpC350Tar267 and the hybrids themselves; fusion sites between McpC and Tar are shown in red and green, respectively. (c–f) Agar plate assays, FRET measurements, and dose–response curves of *E. coli* cells expressing Tar43McpC49Tar184 (c), McpC286Tar200 (d), McpC350Tar267 (e), or McpC350-YSYEH-Tar272 (f) as the sole receptor at the indicated concentrations of L-proline. In the agar plate assays, sites of the ligand source and inoculated cells are shown by a red dotted line and by a yellow dot, respectively. Relative spreading of cells toward or away from the ligand source is indicated. Dose–response curves were analyzed and plotted as in Figure 1.

tricarboxylic acid), the CitA-Tar hybrid Tar43CitA55Tar184 also sensed itaconic acid (EC_{50} = 1.2 ± 0.1 mM) and maleic acid (EC_{50} = 1.0 ± 0.1 mM), which both elicited repellent responses that were opposite to the citrate response (Figure 4e and f and Figure S5d). In contrast, the wild-type Tar and the Tar mutant lacking the periplasmic domain (Tar°-T303I)[51] sensed these two compounds as attractants (Figure S5c and e). The *E. coli* strain deleted for all chemotaxis receptors only showed nonspecific response to these compounds at the highest concentration (Figure S5f). These results suggest that CitA senses these compounds *via* the sensory domain. Interestingly, in this case, the competition experiments showed that adaptation to citrate

DOI: 10.1021/acssynbio.6b00053
ACS Synth. Biol. XXXX, XXX, XXX–XXX

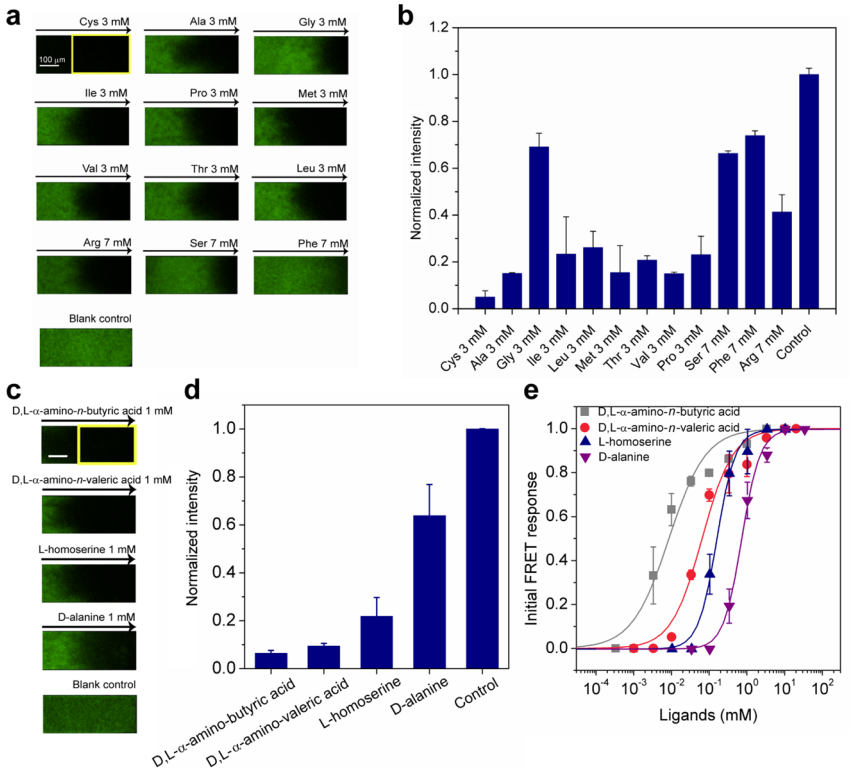

Figure 6. Characterization of ligand specificity of GFP-labeled *E. coli* cells expressing McpC350Tar267 as the sole receptor. (a) Microfluidic assay of the chemotactic response to the indicated amino acids 10 min after ligand addition (scale bar, 100 μm). The arrow on the image indicates the direction up the concentration gradient of each ligand. The highest concentrations of ligands located on the right edge of the observation channel were 3 mM for Cys, Ala, Val, Leu, Ile, Met, Pro, Gly, and Thr, and 7 mM for Arg, Ser, and Phe. The response is characterized by measurements of the fluorescence intensity in the analysis region indicated by a yellow rectangle (300 μm × 200 μm). (b) The corresponding values of the fluorescence intensities in the analysis regions normalized to the fluorescence intensity of cells in buffer. (c, d) Fluorescence microscopic images recorded as in (a) but after 15 min with 1 mM concentrations of indicated compounds (c) and the corresponding response (d). Error bars in b and d indicate the standard errors of 3 replicates. (e) Dose responses of cells expressing McpC350Tar267 to identified novel ligands measured by FRET and analyzed and plotted as in Figure 1.

does not substantially change the responses to itaconic or maleic acids (EC_{50} of 4.1 ± 0.3 mM for itaconic acid and 1.4 ± 0.1 mM for maleic acid, Figure 4e and f), whereas conversely, these two compounds had no effect on the response to citrate (EC_{50} of 5.6 ± 1.6 μM for itaconic acid and 7.1 ± 0.7 μM for maleic acid, Figure 4g). Itaconic and maleic acids could thus interact with the sensory domain of CitA differently from citrate.

Double PDC Domain Hybrid Receptor. The double PDC domain is found in various signaling proteins across a wide range of bacterial species. Several structures of the double PDC domains have been solved,[52] showing that this domain is composed of two Per/ARNT/Sim (PAS)-like $\alpha+\beta$ modules (Figure 5a).[15] The current model of signaling *via* the double PDC domain proposes that the membrane-distal module of the two PDC domains binds a ligand, whereas the membrane-proximal module transmits signals from the distal module to the transmembrane region.[53] The reported hybrids with a double PDC domain include PctA-Tar,[25] PctB-Tar,[25] PctC-Tar,[26] and McpG-Tar[26] with the fusion point after the HAMP domain. In this work, to create a hybrid with a double PDC domain, we used the sensory domain of the amino acid receptor McpC from *B. subtilis* strain 168.[53]

To be able to generalize the method of constructing hybrids with domains different from those found in *E. coli*, we systematically tested different fusion points for the McpC-Tar hybrid. Functional McpC-Tar hybrids were obtained by combining the two receptors in three regions: (1) Tar[1−43]-McpC[49−270]-Tar[184−553] (Tar43McpC49Tar184) with the fusion points above the two TM helices of Tar (Figure 5b and c), (2) McpC[1−286]-Tar[200−553] (McpC286Tar200) with a fusion point in the TM2 of Tar (Figure 5b and d), and (3) McpC[1−350]-Tar[267−553] (McpC350Tar267) with a fusion point after the HAMP domain of McpC/at the beginning of methylation helix of Tar (Figure 5b and e). As before, fusion positions were chosen based on the sequence alignment and secondary structure prediction (Figure 5b) and considering the positions of aromatic anchors for the TM2 sequences (Figure 5b). The repellent responses of these three McpC-Tar hybrids to L-proline, one of the established attractants for McpC,[53] have been confirmed by FRET measurements and semisolid agar plate assays. Neither Tar nor Tar°-T303I showed responses to L-proline (Figure S6). The values of EC_{50} were 68.4 ± 3.4 μM for Tar43McpC49Tar184, 20.3 ± 3.7 μM for McpC286Tar200, and 27.7 ± 7.7 μM for McpC350Tar267 (Figure 5c−e, respectively), comparable to the *in vitro* measured binding affinity of L-proline to McpC (14 μM).[53] All McpC-Tar hybrids showed repellent responses to L-proline, an attractant for *B. subtilis*, consistent with the fact that attractants activate rather than inhibit CheA in *B. subtilis*. The hybrids with fusion points within the HAMP domain, McpC[1−340]-Tar[257−553] (McpC340Tar257), or with the replacement of the protein contact region of McpC with that of Tar, McpC[1−472]-Tar[361−417]-McpC[530−655] (McpC472Tar361McpC530), were also constructed but were nonfunctional, although both of them were well-expressed (Figure S1).

DOI: 10.1021/acssynbio.6b00053
ACS Synth. Biol. XXXX, XXX, XXX−XXX

The outlined strategy of hybrid construction using sequence alignment and structural analysis might not always be successful because some hybrids may adopt unfavorable conformation that abolishes signaling. We thus also explored an alternative strategy that is based on randomizing the sequence at the junction point between the two receptors and then subsequently selecting for functional hybrids. For this, we constructed a library of McpC[1−350]-NNNNN-Tar[272−553] hybrids with a random amino acid linker after the HAMP domain of McpC (Figure 5f). This library was subsequently separated in a gradient of L-proline established on an agar plate, and the constructs that mediated the most efficient spreading down the gradient were selected and identified by DNA sequencing (see Methods and Figure S7). One of the hybrids with the linker Tyr-Ser-Tyr-Glu-His (McpC350-YSYEH-Tar272) sensed L-proline as a repellent. The response was confirmed by the FRET measurement, yielding an EC_{50} of 8.6 ± 2.2 μM (Figure 5f).

Characterizing Ligand Specificity of Hybrid Receptors. Although for our hybrid construction we focused on receptors with known ligands, we think our strategy could be extended to resolve the ligand specificity of the majority of bacterial chemoreceptors and sensory kinases whose ligand remains unknown. We thus propose that hybrid receptors could be used to characterize ligand specificity of various sensory domains in the heterologous *E. coli* system using a previously described microfluidic assay[54] as well as FRET.

Here, we illustrated this approach using example hybrids from McpC (*B. subtilis*) and McpG and McpS (*P. putida*). McpC was reported to sense 17 proteinogenic L-amino acids,[53] 10 of which (Pro, Thr, Gly, Ser, Val, Ala, Tyr, Ile, Phe, and Leu) were confirmed to bind to the ligand-binding pocket by isothermal titration calorimetry (ITC).[53] We thus tested response of the GFP-labeled *E. coli* strain UU1250 expressing McpC350Tar267 to all 20 proteinogenic L-amino acids using microfluidics. This strain indeed showed a robust repellent response to 12 amino acids (Cys, Val, Ala, Pro, Ile, Leu, Thr, Gly, Ser, Phe, Met, and Arg) (Figure 6a), which resulted in a decreased number of fluorescent cells near the top of the gradient (Figure 6b). We could thus confirm McpC-mediated responses to 9 of the 10 amino acids, which show both binding affinities in ITC and chemotaxis (Pro, Thr, Gly, Ser, Val, Ala, Ile, Phe, and Leu). *E. coli* expressing McpC350Tar267 further responded to Met, Arg, and Cys, which are putative McpC ligands that could not be detected or measured by ITC.[53] Encouraged by these results, we applied the assay to screen for novel ligands of McpC using the BIOLOG library of compounds that can serve as a microbial carbon or nitrogen source (Table S2). Because compound concentrations in the BIOLOG library are not defined, the candidate compounds that elicited the McpC350Tar267-specific responses were verified again by microfluidics and FRET. We found that D,L-α-amino-*n*-butyric acid, D,L-α-amino-*n*-valeric acid, L-homoserine, and D-alanine are potent ligands for McpC (Figure 6c−e and Figure S8). Tar showed either no response or a much weaker response to these compounds in microfluidics and FRET (Figure S9). The chemical structures of the compounds and EC_{50} values obtained by FRET are shown in Table 1.

We also identified novel ligands of McpG and McpS using a previously reported McpG-Tar hybrid McpG[1−348]-Tar[268−553] (McpG348Tar268)[26] and McpS295Tar200, respectively (Tables S3 and S4, respectively). We found that besides its previously established ligand γ-aminobutyrate (GABA),[26] McpG senses agmatine, putrescine, L-proline, L-homoserine, L-alanine, L-cysteine, and ethylenediamine (Figure 7a−c, Figure S10, and Table 1), whereas McpS senses L-aspartate, itaconic acid, D-tartaric acid, α-hydroxy-glutaric acid-γ-lactone, caproic acid, and valeric acid as novel attractants (Figure 7d−f, Figure S11, and Table 1). The wild-type Tar or Tar°-T303I showed no response or much weaker responses to these compounds[6] (Figure S9).

Table 1. Novel Ligands for McpC, McpG, and McpS

Name	Structure	EC_{50}
McpC		
D,L-α-amino-*n*-butyric acid		8.6 ± 2.4 μM
D,L-α-amino-*n*-valeric acid		64.6 ± 12.5 μM
L-homoserine		154 ± 13 μM
D-alanine		703 ± 44 μM
McpG		
Agmatine	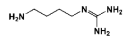	2.3 ± 0.3 μM
Putrescine	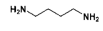	27.5 ± 5.5 μM
L-proline		59.6 ± 4.5 μM
L-homoserine		98.5 ± 6.4 μM
L-alanine		20.9 ± 1.8 μM
L-cysteine		28.5 ± 1.0 μM
Ethylenediamine		9.8 ± 0.6 μM
McpS		
L-aspartate		1.8 ± 0.3 μM
Itaconic acid		83.5 ± 5.1 μM
Caproic acid	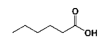	9.9 ± 2.1 μM
D-tartaric acid		9.3 ± 0.4 μM
α-Hydroxy-glutaric acid -γ-lactone		146 ± 6 μM
Valeric acid		52.8 ± 6.1 μM

DISCUSSION

Construction of hybrid sensors in bacteria is a potentially powerful tool for characterizing the ligand specificity of novel sensory domains as well as constructing bacterial biosensors. Although several such hybrids were previously reported,[2,6,25−27] the principles for making functional hybrids and the flexibility allowed in combining receptors with structurally different sensory domains remained unknown. In this work, we have shown that most structural types of extracellular sensory domains found in chemotaxis receptors or HKs (the four-helix bundle, HBM, NIT, single PDC, and double PDC domain) can successfully be fused to the *E. coli* chemotaxis receptor Tar. The majority of the constructed hybrids were functional, impressively demonstrating functional modularity of bacterial

DOI: 10.1021/acssynbio.6b00053
ACS Synth. Biol. XXXX, XXX, XXX−XXX

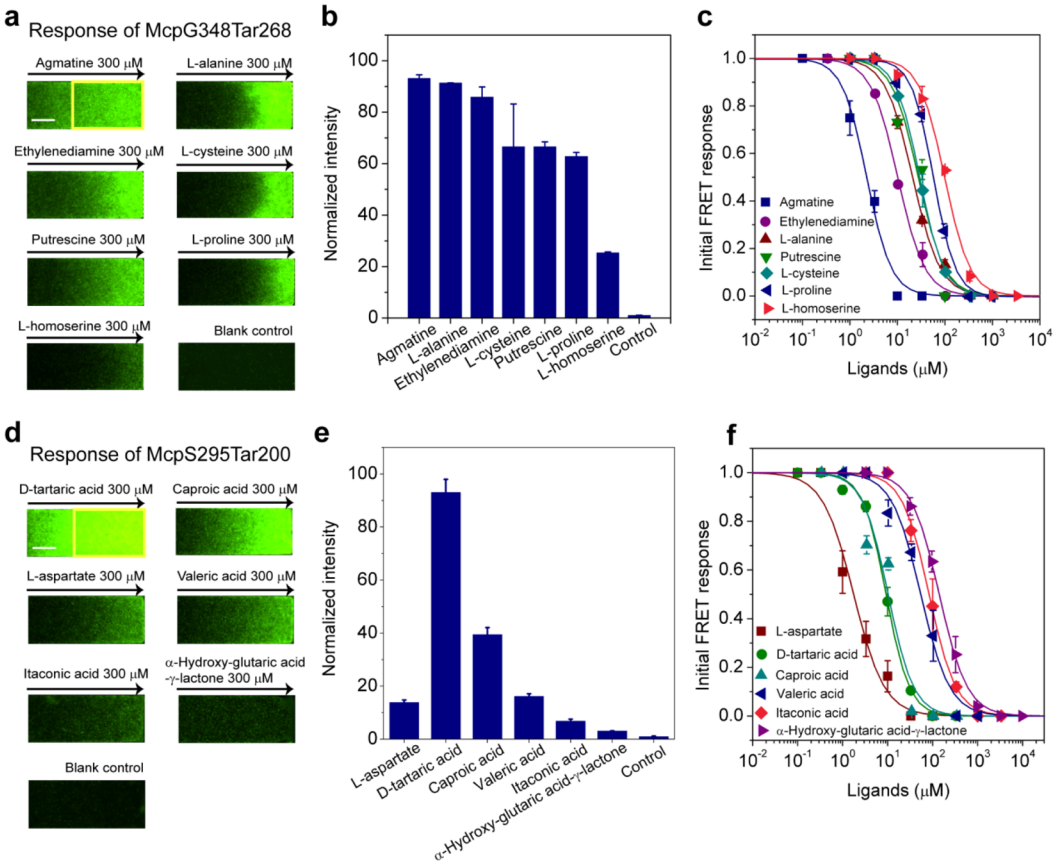

Figure 7. Characterization of ligand specificity of GFP-labeled *E. coli* cells expressing McpG348Tar268 or McpS295Tar200 as the sole receptor. (a) Microfluidic assay of the response of McpG348Tar268 to the novel ligands 30 min after ligand addition (scale bar, 100 μm). The arrow on the image indicates the direction up the concentration gradient of each ligand. The highest concentration of ligand located on the right edge of the observation channel was 300 μM. (b) The corresponding values of the fluorescence intensities in the analysis regions normalized to the fluorescence intensity of cells in buffer. (c) Dose responses of cells expressing McpG348Tar268 to identified novel ligands measured by FRET. (d, e) Fluorescence microscopic images recorded as in a for McpS295Tar200 responding to 300 μM of the indicated compounds (d) and corresponding response (e). Error bars in b and e indicate the standard errors of 3 replicates. (f) Dose responses of cells expressing McpS295Tar200 to identified novel ligands measured by FRET and analyzed and plotted as in Figure 1.

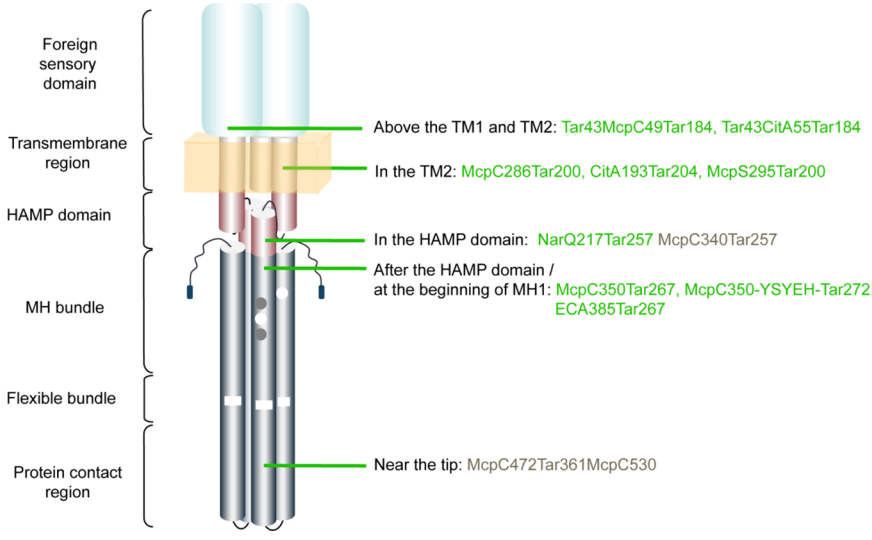

Figure 8. Overview of hybrid receptors and corresponding fusion sites tested in this study. Functional hybrids are shown in green, and the nonfunctional hybrids are indicated in gray.

receptors. Our results indicate that, potentially, any existing sensory and signaling domain can be artificially combined to produce a functional sensor.

We could further establish some general guidelines for making functional receptor hybrids. In general, positions that are located (i) above the two TM helices, (ii) within the TM2 helix, or (iii)

DOI: 10.1021/acssynbio.6b00053
ACS Synth. Biol. XXXX, XXX, XXX−XXX

after the HAMP domain appear to be the most promising (Figure 8). In the first case, it is important to choose the correct position where the N- and C-terminals of the foreign domain could be connected to the two TM helices of the other receptor. Here, we show that even in the absence of any sequence or structural homology, fusion points could be identified based on the hydrophilic or hydrophobic properties of the residues, as in the case of Tar43CitA55Tar184. The aromatic anchors at the beginning and/or the end of the TM2 helix can also guide the alignment for the fusions within TM2. Although conservation of sensory and HAMP domains facilitates alignment of sequences belonging to different receptors, fusion strategies (i–ii) are apparently applicable even for HKs that do not possess a HAMP domain. Finally, the region after the HAMP domain can also serve as a proper fusion point because the mechanism of signal transduction through HAMP domains might be conserved in chemotaxis receptors and HKs.[2] The ability to achieve a functional receptor hybrid with fusion sites within the HAMP domain appears to be more sensitive to the sequence because the hybrid NarQ217Tar257 was functional whereas McpC340Tar257 was not. Finally, we showed that, besides targeting specific fusion points, the random-linker approach might also be employed, which relies on selection of the hybrid(s) with the desired activity from the library.

Notably, functionality of bacterial chemoreceptor hybrids might be aided by the receptor methylation system. Although this system normally compensates for changes in the receptor activity that result from ligand binding, it is likely to also partly compensate for conformational shifts that result from hybrid construction and bias receptors toward either an active or inactive state.

One possible application of hybrid receptors is to characterize ligand specificity of a target receptor/HK, addressing a huge gap that exists between thousands of sequenced receptor and HK genes and only a very limited number of receptors/HKs for which the ligand specificity has been established. To illustrate this approach, we have identified novel ligands for McpG and McpS from *P. putida* and McpC from *B. subtilis*. Here, we used microfluidic experiments and agar plate assays for the initial screening and FRET for subsequent detailed characterization of ligand specificity with all of these assays showing consistent results. We found that, besides its established ligand GABA, McpG also senses agmatine, putrescine, L-proline, L-cysteine, L-alanine, ethylenediamine, and L-homoserine as attractants. L-aspartate, itaconic acid, D-tartaric acid, α-hydroxy-glutaric acid-γ-lactone, caproic acid, and valeric acid are novel attractants for McpS. In addition to 12 proteinogenic amino acids (Cys, Val, Ala, Pro, Ile, Leu, Thr, Gly, Ser, Phe, Met, and Arg), McpC senses D,L-α-amino-*n*-butyric acid, D,L-α-amino-*n*-valeric acid, L-homoserine, and D-alanine as novel ligands. These compounds may be used as energy sources or as biological precursors. Moreover, L-proline, L-homoserine, and putrescine are abundant in plant exudates and might be used by *P. putida* and *B. subtilis* as cues to locate plants in the soil where both species are found.

This approach can also be applied for identifying ligands of HKs. Here, we determined two novel ligands for CitA: itaconic and maleic acids. Interestingly, these ligands have opposite effects on the activity of the hybrid, suggesting that they might counteract the action of citrate. Additionally, our data suggests that their mode of binding to CitA is different from that of citrate. We also identified nitrite as a secondary ligand of NarQ, in which case the binding was competitive with the established ligand nitrate.

In conclusion, we have developed here a general strategy for creating functional hybrid chemotaxis receptors, which enabled us to make fusions between the cytoplasmic domain of the *E. coli* receptor Tar and every tested sensory domain from other chemotaxis receptors or histidine kinases. Importantly, the design of such functional hybrids required neither sequence nor structural homology with the sensory domain of Tar. Given the immense diversity of the sensory domains in bacteria and archaea that detect various small molecules, such hybrids potentially provide a rich source of novel bacterial biosensors. Among the sensory domains studied in this work, the PAS-like domains appear to have an exceptionally broad range of specificity, consistent with their ubiquitous presence in both bacterial and eukaryotic signaling proteins,[55] and may thus represent particularly attractive targets for the biosensor design. Moreover, because with our current design the hybrids control the chemotaxis system of *E. coli*, a number of standardized chemotaxis assays can be used to characterize the specificity of the sensory domains, including quantification of relative affinities for proposed ligands and screening for novel ligands of chemotaxis receptors and HKs.

METHODS

Strains and Plasmids. Bacterial strains and plasmids used in this work are listed in Table S1. For the FRET measurements, receptorless *cheY cheZ* strain VS181 [Δ(*cheYcheZ*)Δ*aer*Δ*tsr*Δ(*tar-tap*)Δ*trg*][39] was transformed with the plasmid pVS88[39] expressing FRET pair CheY-YFP/CheZ-CFP and a plasmid expressing the receptor of interest. For the agar plate assay, receptorless strain UU1250 [Δ*aer*Δ*tsr*Δ(*tar-tap*)Δ*trg*][43] was transformed with a plasmid expressing a particular receptor. For the microfluidic experiments, the same strain was additionally transformed with the plasmid expressing GFP. Chemoreceptor and HK hybrids were constructed as described in the text. The expression of all full-length hybrids was confirmed by immunoblotting using *E. coli cheR cheB* strain VH1 [Δ(*cheRcheB*)Δ(*cheYcheZ*)Δ*aer*Δ*tsr*Δ(*tar-tap*)Δ*trg*].[56]

Molecular Cloning. The plasmids pSB1 to pSB11 were constructed to express the hybrid receptors. The coding sequence of each hybrid was amplified using PCR reaction. Two oligonucleotides introduced restriction sites *Nde*I at the 5′-end and *BamH*I at the 3′-end. The amplified fragment was digested and ligated with the plasmid pKG116.[37] The Tar portions of pSB1 and pSB7 were amplified using pPA791. For plasmid pSB10, a *Not*I restriction site was introduced in the TM2 region to connect the fragment of McpS with that of Tar, which replaced the Tar residues $[VVV]_{200-202}$ to $[AAA]_{200-202}$.

FRET Measurements. Preparation of cells for FRET measurements was described previously.[38] In short, *E. coli* cells expressing the receptor of interest were grown in TB (1% tryptone, 0.5% NaCl) supplemented with antibiotics (100 μg mL^{-1} of ampicillin; 17 μg mL^{-1} of chloramphenicol) and appropriate inducers at 34 °C and 275 rpm. Cells were harvested at OD_{600} of 0.6 and washed twice with the tethering buffer (10 mM KH_2PO_4/K_2HPO_4, 0.1 mM EDTA, 1 μM methionine, 10 mM sodium lactate, pH 7.0). FRET measurements were performed on an upright fluorescence microscope (Zeiss Axio Imager.Z1). Strains expressing receptors were stimulated with compounds of interest. The fluorescence signals were recorded, analyzed as described previously,[38] and plotted using KaleidaGraph (Synergy Software). Data were fit to a Hill model. For the repellent response, $Y = A \times L^H/(L^H + K^H)$, whereas for the attractant response, $Y = A \times (1 - L^H/(L^H + K^H))$. In the model, Y

DOI: 10.1021/acssynbio.6b00053
ACS Synth. Biol. XXXX, XXX, XXX–XXX

is the initial FRET response, L is the concentration of the ligand, A is the amplitude (for the saturated response, A is fixed to be 1), H is the Hill coefficient, and K is the EC_{50}.

Agar Plate Assay. Minimal A agar (0.25% agar, 10 mM KH_2PO_4/K_2HPO_4, 8 mM $(NH_4)_2SO_4$, 2 mM citrate, 1 mM $MgSO_4$, 0.1 mg mL^{-1} of thiamine-HCl, 1 mM glycerol, and 40 μg mL^{-1} of a mixture of threonine, methionine, leucine, and histidine) supplemented with antibiotics and inducers was used for the agar plate assay. Chemical solutions were applied to the center line of the plate and incubated at 4 °C for 12−16 h to generate a chemical gradient.[20] Overnight cultures expressing the receptor of interest were washed twice with tethering buffer and applied to the plate at a defined distance from the line where the chemical was inoculated: 2.5 cm for McpC-Tar, 2 cm for CitA-Tar, and 3.5 cm for McpS-Tar. Plates were incubated at 30 °C for 24−48 h.

For selecting a functional McpC-Tar hybrid with a random linker, the library was applied to an agar plate for the first round of selection. Cells that had the best repellent responses to L-proline, which was applied to the center, accumulated at the edge of the plate. These cells were then selected and grown in LB medium and inoculated on another plate for the second round of selection. After three rounds of selection, the most chemotactic cells were streaked out on LB plates to obtain single colonies. The plasmids were extracted from these colonies and transformed again to UU1250. The chemotaxis behavior of the selected McpC-Tar hybrid was confirmed again on agar plates. The sequence of the linker in the functional hybrid was identified by DNA sequencing.

Microfluidic Experiments. *E. coli* UU1250-expressing hybrid receptors and GFP proteins were grown at 34 °C in TB supplemented with antibiotics and inducers until the OD_{600} reached 0.6. Cells were harvested by centrifugation at 3,000 rpm for 3 min and washed twice with the tethering buffer. The compounds supplied from BIOLOG were dissolved in 50 μL of water to reach a final concentration of 10−20 mM.[57,58] The other compounds were dissolved in the tethering buffer and adjusted to pH 7.0. The responses of *E. coli* cells to concentration gradients of the various compounds were measured using a microfluidic device as previously described.[54] In summary, *E. coli* cells were added at the sink side pore of the device to a final OD_{600} of 1.2−2 and equilibrated for 40 min in the observation channel. Compound solutions were added at the source side pore and allowed to diffuse into the observation channel for an indicated time to establish a concentration gradient. Fluorescence microscopy on a Nikon Ti-E microscope system with a 20× objective lens was used to detect the fluorescence intensity of cells in the observation channel. Cellular response was characterized by the fluorescence intensity in the analysis region (300 μm × 200 μm) of the observation channel. Data were analyzed using ImageJ (Wayne Rasband, National Institutes of Health, USA).

Immunoblotting. Immunoblotting was performed as described before.[19] Briefly, cells were grown and prepared as for FRET measurements. Culture samples were concentrated 17-fold, and 10 μL of the sample was separated using 12% SDS-PAGE. Rabbit polyclonal anti-Tar antibody was used as the primary antibody, and fluorescently labeled goat antirabbit IgG IRDye 800 conjugate was used as the secondary antibody. A LI-COR Odyssey Infrared Imaging System was used for detection. Band intensities were quantified using ImageJ.

■ ASSOCIATED CONTENT

Supporting Information

The Supporting Information is available free of charge on the ACS Publications website at DOI: 10.1021/acssynbio.6b00053.

Additional experimental data and results: Supplementary Figures S1−S11, Supplementary Tables S1−S4, and Supplementary References (PDF)

■ AUTHOR INFORMATION

Corresponding Author

*E-mail: victor.sourjik@synmikro.mpi-marburg.mpg.de. Tel.: (+49) 6421 28 21400. Fax: (+49) 6421 28 21485.

Author Contributions

V.S. designed the research; S.B., A.M.P., Y.Y., and F.J. performed the research and analyzed data, and S.B. and V.S. wrote the paper.

Notes

The authors declare no competing financial interest.

■ ACKNOWLEDGMENTS

We would like to thank Prof. Birte Höcker (MPI for Developmental Biology, Tuebingen, Germany) for helpful discussion, and Dr. Chunxiong Luo and Xi Chen (Peking University, Beijing, China) for providing the microfluidic device. This work was partly supported by grant 294761-MicRobE from the European Research Council and by grant SO 421/11-1 from the Deutsche Forschungsgemeinschaft.

■ REFERENCES

(1) Sourjik, V., and Wingreen, N. S. (2012) Responding to chemical gradients: bacterial chemotaxis. *Curr. Opin. Cell Biol. 24*, 262−268.

(2) Salis, H., Tamsir, A., and Voigt, C. (2009) Engineering bacterial signals and sensors. *Contrib. Microbiol. 16*, 194−225.

(3) Wadhams, G. H., and Armitage, J. P. (2004) Making sense of it all: bacterial chemotaxis. *Nat. Rev. Mol. Cell Biol. 5*, 1024−1037.

(4) Szurmant, H., and Ordal, G. W. (2004) Diversity in chemotaxis mechanisms among the bacteria and archaea. *Microbiol. Mol. Biol. Rev. 68*, 301−319.

(5) Hazelbauer, G. L. (2012) Bacterial chemotaxis: the early years of molecular studies. *Annu. Rev. Microbiol. 66*, 285−303.

(6) Yang, Y., Pollard, A. M., Hofler, C., Poschet, G., Wirtz, M., Hell, R., and Sourjik, V. (2015) Relation between chemotaxis and consumption of amino acids in bacteria. *Mol. Microbiol. 96*, 1272−1282.

(7) Hegde, M., Englert, D. L., Schrock, S., Cohn, W. B., Vogt, C., Wood, T. K., Manson, M. D., and Jayaraman, A. (2011) Chemotaxis to the quorum-sensing signal AI-2 requires the Tsr chemoreceptor and the periplasmic LsrB AI-2-binding protein. *J. Bacteriol. 193*, 768−773.

(8) Parales, R. E., Luu, R. A., Hughes, J. G., and Ditty, J. L. (2015) Bacterial chemotaxis to xenobiotic chemicals and naturally-occurring analogs. *Curr. Opin. Biotechnol. 33*, 318−326.

(9) Adler, B., and de la Pena Moctezuma, A. (2010) Leptospira and leptospirosis. *Vet. Microbiol. 140*, 287−296.

(10) Parkinson, J. S., Hazelbauer, G. L., and Falke, J. J. (2015) Signaling and sensory adaptation in *Escherichia coli* chemoreceptors: 2015 update. *Trends Microbiol. 23*, 257−266.

(11) Hazelbauer, G. L., and Lai, W. C. (2010) Bacterial chemoreceptors: providing enhanced features to two-component signaling. *Curr. Opin. Microbiol. 13*, 124−132.

(12) Hazelbauer, G. L., Falke, J. J., and Parkinson, J. S. (2008) Bacterial chemoreceptors: high-performance signaling in networked arrays. *Trends Biochem. Sci. 33*, 9−19.

(13) Lacal, J., Garcia-Fontana, C., Munoz-Martinez, F., Ramos, J. L., and Krell, T. (2010) Sensing of environmental signals: classification of chemoreceptors according to the size of their ligand binding regions. *Environ. Microbiol. 12*, 2873−2884.

DOI: 10.1021/acssynbio.6b00053
ACS Synth. Biol. XXXX, XXX, XXX−XXX

(14) Ulrich, L. E., and Zhulin, I. B. (2005) Four-helix bundle: a ubiquitous sensory module in prokaryotic signal transduction. *Bioinformatics 21* (Suppl 3), iii45−48.
(15) Cheung, J., and Hendrickson, W. A. (2010) Sensor domains of two-component regulatory systems. *Curr. Opin. Microbiol. 13*, 116−123.
(16) Ortega, A., and Krell, T. (2014) The HBM domain: introducing bimodularity to bacterial sensing. *Protein Sci. 23*, 332−336.
(17) Shu, C. J., Ulrich, L. E., and Zhulin, I. B. (2003) The NIT domain: a predicted nitrate-responsive module in bacterial sensory receptors. *Trends Biochem. Sci. 28*, 121−124.
(18) Bi, S., and Lai, L. (2015) Bacterial chemoreceptors and chemoeffectors. *Cell. Mol. Life Sci. 72*, 691−708.
(19) Bi, S., Yu, D., Si, G., Luo, C., Li, T., Ouyang, Q., Jakovljevic, V., Sourjik, V., Tu, Y., and Lai, L. (2013) Discovery of novel chemoeffectors and rational design of *Escherichia coli* chemoreceptor specificity. *Proc. Natl. Acad. Sci. U. S. A. 110*, 16814−16819.
(20) Derr, P., Boder, E., and Goulian, M. (2006) Changing the specificity of a bacterial chemoreceptor. *J. Mol. Biol. 355*, 923−932.
(21) Yang, Y., and Sourjik, V. (2012) Opposite responses by different chemoreceptors set a tunable preference point in *Escherichia coli* pH taxis. *Mol. Microbiol. 86*, 1482−1489.
(22) Feng, X., Baumgartner, J. W., and Hazelbauer, G. L. (1997) High- and low-abundance chemoreceptors in *Escherichia coli*: differential activities associated with closely related cytoplasmic domains. *J. Bacteriol. 179*, 6714−6720.
(23) Weerasuriya, S., Schneider, B. M., and Manson, M. D. (1998) Chimeric chemoreceptors in *Escherichia coli*: signaling properties of Tar-Tap and Tap-Tar hybrids. *J. Bacteriol. 180*, 914−920.
(24) Kristich, C. J., Glekas, G. D., and Ordal, G. W. (2003) The conserved cytoplasmic module of the transmembrane chemoreceptor McpC mediates carbohydrate chemotaxis in *Bacillus subtilis*. *Mol. Microbiol. 47*, 1353−1366.
(25) Reyes-Darias, J. A., Yang, Y., Sourjik, V., and Krell, T. (2015) Correlation between signal input and output in PctA and PctB amino acid chemoreceptor of *Pseudomonas aeruginosa*. *Mol. Microbiol. 96*, 513−525.
(26) Reyes-Darias, J. A., Garcia, V., Rico-Jimenez, M., Corral-Lugo, A., Lesouhaitier, O., Juarez-Hernandez, D., Yang, Y., Bi, S., Feuilloley, M., Munoz-Rojas, J., Sourjik, V., and Krell, T. (2015) Specific gamma-aminobutyrate chemotaxis in *pseudomonads* with different lifestyle. *Mol. Microbiol. 97*, 488−501.
(27) Ward, S. M., Delgado, A., Gunsalus, R. P., and Manson, M. D. (2002) A NarX-Tar chimera mediates repellent chemotaxis to nitrate and nitrite. *Mol. Microbiol. 44*, 709−719.
(28) Xu, Q., Black, W. P., Mauriello, E. M., Zusman, D. R., and Yang, Z. (2007) Chemotaxis mediated by NarX-FrzCD chimeras and non-adapting repellent responses in *Myxococcus xanthus*. *Mol. Microbiol. 66*, 1370−1381.
(29) Milburn, M. V., Prive, G. G., Milligan, D. L., Scott, W. G., Yeh, J., Jancarik, J., Koshland, D. E., Jr., and Kim, S. H. (1991) Three-dimensional structures of the ligand-binding domain of the bacterial aspartate receptor with and without a ligand. *Science 254*, 1342−1347.
(30) Tajima, H., Imada, K., Sakuma, M., Hattori, F., Nara, T., Kamo, N., Homma, M., and Kawagishi, I. (2011) Ligand specificity determined by differentially arranged common ligand-binding residues in bacterial amino acid chemoreceptors Tsr and Tar. *J. Biol. Chem. 286*, 42200−42210.
(31) Pham, H. T., and Parkinson, J. S. (2011) Phenol sensing by *Escherichia coli* chemoreceptors: a nonclassical mechanism. *J. Bacteriol. 193*, 6597−6604.
(32) Krikos, A., Conley, M. P., Boyd, A., Berg, H. C., and Simon, M. I. (1985) Chimeric chemosensory transducers of *Escherichia coli*. *Proc. Natl. Acad. Sci. U. S. A. 82*, 1326−1330.
(33) Umemura, T., Matsumoto, Y., Ohnishi, K., Homma, M., and Kawagishi, I. (2002) Sensing of cytoplasmic pH by bacterial chemoreceptors involves the linker region that connects the membrane-spanning and the signal-modulating helices. *J. Biol. Chem. 277*, 1593−1598.
(34) Cheung, J., and Hendrickson, W. A. (2009) Structural analysis of ligand stimulation of the histidine kinase NarX. *Structure 17*, 190−201.
(35) Kaiser, M., and Sawers, G. (1995) Nitrate repression of the *Escherichia coli* pfl operon is mediated by the dual sensors NarQ and NarX and the dual regulators NarL and NarP. *J. Bacteriol. 177*, 3647−3655.
(36) Thompson, J. D., Higgins, D. G., and Gibson, T. J. (1994) CLUSTAL W: improving the sensitivity of progressive multiple sequence alignment through sequence weighting, position-specific gap penalties and weight matrix choice. *Nucleic Acids Res. 22*, 4673−4680.
(37) Buron-Barral, M. C., Gosink, K. K., and Parkinson, J. S. (2006) Loss- and gain-of-function mutations in the F1-HAMP region of the *Escherichia coli* aerotaxis transducer Aer. *J. Bacteriol. 188*, 3477−3486.
(38) Sourjik, V., and Berg, H. C. (2002) Receptor sensitivity in bacterial chemotaxis. *Proc. Natl. Acad. Sci. U. S. A. 99*, 123−127.
(39) Sourjik, V., and Berg, H. C. (2004) Functional interactions between receptors in bacterial chemotaxis. *Nature 428*, 437−441.
(40) Neumann, S., Hansen, C. H., Wingreen, N. S., and Sourjik, V. (2010) Differences in signalling by directly and indirectly binding ligands in bacterial chemotaxis. *EMBO J. 29*, 3484−3495.
(41) Pineda-Molina, E., Reyes-Darias, J. A., Lacal, J., Ramos, J. L., Garcia-Ruiz, J. M., Gavira, J. A., and Krell, T. (2012) Evidence for chemoreceptors with bimodular ligand-binding regions harboring two signal-binding sites. *Proc. Natl. Acad. Sci. U. S. A. 109*, 18926−18931.
(42) Lacal, J., Alfonso, C., Liu, X., Parales, R. E., Morel, B., Conejero-Lara, F., Rivas, G., Duque, E., Ramos, J. L., and Krell, T. (2010) Identification of a chemoreceptor for tricarboxylic acid cycle intermediates: differential chemotactic response towards receptor ligands. *J. Biol. Chem. 285*, 23126−23136.
(43) Ames, P., Studdert, C. A., Reiser, R. H., and Parkinson, J. S. (2002) Collaborative signaling by mixed chemoreceptor teams in *Escherichia coli*. *Proc. Natl. Acad. Sci. U. S. A. 99*, 7060−7065.
(44) Boudes, M., Lazar, N., Graille, M., Durand, D., Gaidenko, T. A., Stewart, V., and van Tilbeurgh, H. (2012) The structure of the NasR transcription antiterminator reveals a one-component system with a NIT nitrate receptor coupled to an ANTAR RNA-binding effector. *Mol. Microbiol. 85*, 431−444.
(45) Letunic, I., Doerks, T., and Bork, P. (2015) SMART: recent updates, new developments and status in 2015. *Nucleic Acids Res. 43*, D257−260.
(46) Cheung, J., Bingman, C. A., Reyngold, M., Hendrickson, W. A., and Waldburger, C. D. (2008) Crystal structure of a functional dimer of the PhoQ sensor domain. *J. Biol. Chem. 283*, 13762−13770.
(47) Cheung, J., and Hendrickson, W. A. (2008) Crystal structures of C4-dicarboxylate ligand complexes with sensor domains of histidine kinases DcuS and DctB. *J. Biol. Chem. 283*, 30256−30265.
(48) Sevvana, M., Vijayan, V., Zweckstetter, M., Reinelt, S., Madden, D. R., Herbst-Irmer, R., Sheldrick, G. M., Bott, M., Griesinger, C., and Becker, S. (2008) A ligand-induced switch in the periplasmic domain of sensor histidine kinase CitA. *J. Mol. Biol. 377*, 512−523.
(49) Kaspar, S., and Bott, M. (2002) The sensor kinase CitA (DpiB) of *Escherichia coli* functions as a high-affinity citrate receptor. *Arch. Microbiol. 177*, 313−321.
(50) McGuffin, L. J., Bryson, K., and Jones, D. T. (2000) The PSIPRED protein structure prediction server. *Bioinformatics 16*, 404−405.
(51) Gosink, K. K., Buron-Barral, M. C., and Parkinson, J. S. (2006) Signaling interactions between the aerotaxis transducer Aer and heterologous chemoreceptors in *Escherichia coli*. *J. Bacteriol. 188*, 3487−3493.
(52) Zhang, Z., and Hendrickson, W. A. (2010) Structural characterization of the predominant family of histidine kinase sensor domains. *J. Mol. Biol. 400*, 335−353.
(53) Glekas, G. D., Mulhern, B. J., Kroc, A., Duelfer, K. A., Lei, V., Rao, C. V., and Ordal, G. W. (2012) The *Bacillus subtilis* chemoreceptor McpC senses multiple ligands using two discrete mechanisms. *J. Biol. Chem. 287*, 39412−39418.

DOI: 10.1021/acssynbio.6b00053
ACS Synth. Biol. XXXX, XXX, XXX−XXX

(54) Si, G., Yang, W., Bi, S., Luo, C., and Ouyang, Q. (2012) A parallel diffusion-based microfluidic device for bacterial chemotaxis analysis. *Lab Chip 12*, 1389−1394.
(55) Henry, J. T., and Crosson, S. (2011) Ligand-binding PAS domains in a genomic, cellular, and structural context. *Annu. Rev. Microbiol. 65*, 261−286.
(56) Oleksiuk, O., Jakovljevic, V., Vladimirov, N., Carvalho, R., Paster, E., Ryu, W. S., Meir, Y., Wingreen, N. S., Kollmann, M., and Sourjik, V. (2011) Thermal robustness of signaling in bacterial chemotaxis. *Cell 145*, 312−321.
(57) McKellar, J. L., Minnell, J. J., and Gerth, M. L. (2015) A high-throughput screen for ligand binding reveals the specificities of three amino acid chemoreceptors from *Pseudomonas syringae* pv. *actinidiae*. *Mol. Microbiol. 96*, 694−707.
(58) Krell, T. (2015) Tackling the bottleneck in bacterial signal transduction research: high-throughput identification of signal molecules. *Mol. Microbiol. 96*, 685−688.

DOI: 10.1021/acssynbio.6b00053
ACS Synth. Biol. XXXX, XXX, XXX−XXX